Chapter 1. Introduction of titanium oxides: properties and synthesis

1.1. Two of new centurial challenges: environmental protections and energy sources

After industrial revolution of 18th century, the world populations have increased by a wide margin (figure 1.1). The problems incident to the population explosion are environmental pollutions and scarcity of energy. Recently, radical changes of climate go with greenhouse effect and soared petroleum price caused great costs repeatedly. The pollutions of water and air also become more and more serious; the reports about the warning of pollutants menace people health are published constantly. The difficulties of environment and energy become obstacles to the progress of our species, finding the solution is of great urgency.

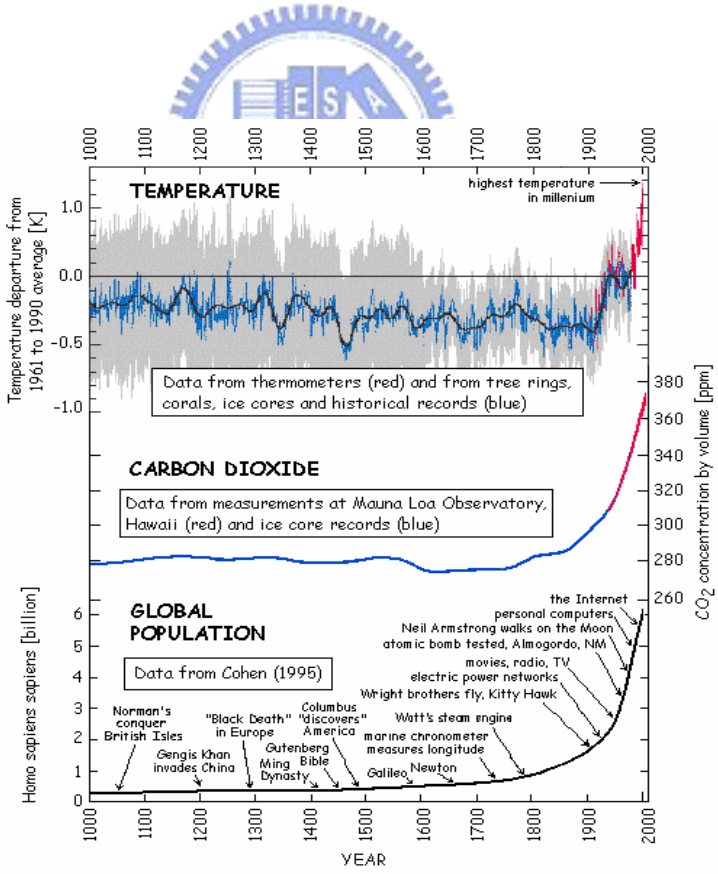

Figure 1.1. Correlations of global population and greenhouse effect.

The development of solar energy related application provides a good answer to the problem mentioned above, for example, we can employ photobattery to instead of oil, and photocatalysis to clarify pollutants. However, there still are many technical thresholds waiting for overcome. How to find a better energy conversion efficient and economic material is many scientists' ambition. Among the known materials, titanium oxides and derives are regarded as powerful candidate due to its non toxic, low cost, abundance, good photo-electric-chemical properties and multi-functional applications (see figure 1.2).

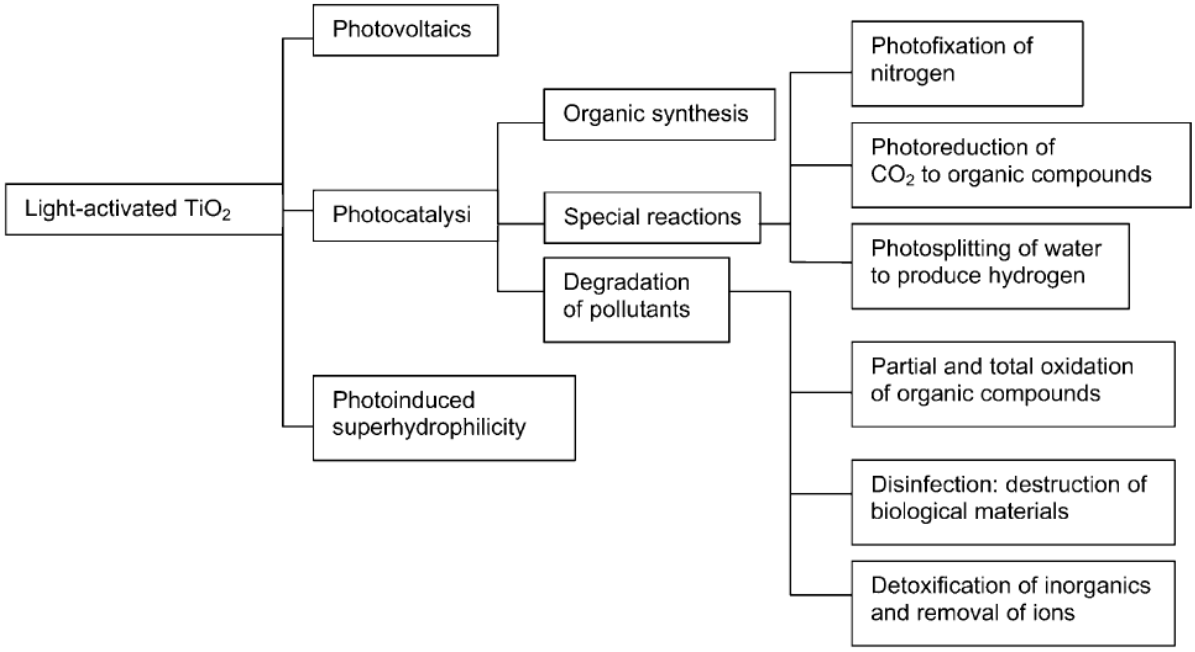

Figure 1.2. Photoinduced processes on TiO_2.[1]

1.2. Background, Applications and Synthesis of Titanium Dioxides

1.2.1. Titanium in Our World [1]

Titanium is the ninth most abundant element (constitution ~ 0.63% of the Earth's crust)

and the fourth most abundant metal in this world. It was discovered in 1791 in England by Reverend William Gregor in ilmenite as a new element. This element was rediscovered by the German chemist Heinrich Klaporth in rutile ore several years later, and he named it Titans, first sons of the goddess in Greek mythology.

Titanium exists primarily in minerals titanates and many iron ores, like rutile, ilmenite, leucoxene, anatase, brookite, perovskite and sphene. It was also detected in meteorites, the rocks brought back from moon and Sun. Mineral sources of TiO_2 are rutile, ilmenite, and leucoxene (a weathering product from ilmenite). About 98% of the world's production is used to make white pigments, and there is only 2% used as titanium metal, welding rod coatings, fluxes, and other products.

1.2.2. Various Allotropes of TiO_2[102,103]

Until now, there are seven kinds of allotropes of TiO_2 discovered, inclusive of TiO_2(B),[2,3] anatase,[4,5] rutile,[6,7] hollandite,[8] ramsdellite,[9] brookite[10] and TiO_2 type α-PbO_2 (or called TiO_2-II).[11,12] Anatase, brookite, rutile and TiO_2(B) are the four commoner structures which can be found in nature. The TiO_2-II, hollandite and ramsdellite are higher pressure forms starting from rutile.[8,9,11] These TiO_2 structures can be discussed in terms of TiO_6 octahedrons which is composed of one central titanium atom and six coordinated oxygen atoms. They are assembled to 3D crystal as association of octahedral chains by sharing corner or edge oxygen. The different condensations result variousness of TiO_2 allotropes, we can describe the various structures as some special chain units. The lattice parameters of these TiO_2 allotropes are in table 1.1. In the following, we represent each structure with different viewing directions of lattice axes.

Table 1.1. Lattice parameters of various allotropes of TiO_2.

common name	a (Å)	b (Å)	c (Å)	β (°)	system	space group
TiO_2(B)	12.163(5)	3.735(2)	6.513(2)	107.29(5)	monoclinic	C2/*m*
TiO_2-anatase	3.785(4)		9.514(1)		tetragonal	I4_1/*amd*
TiO_2-rutile	4.594(2)		2.9586(2)		tetragonal	P4_2/*mnm*
TiO_2-hollandite	10.182(1)		2.966(1)		tetragonal	I4/*m*
TiO_2-ramsdellite	4.9022(14)	9.4590(12)	2.9583(14)		orthorhombic	P*bnm*
TiO_2-brookite	9.191(4)	5.463(4)	5.157(4)		orthorhombic	P*bca*
TiO_2 type α-PbO_2	4.531(2)	5.498(1)	4.900(4)		orthorhombic	P*bcn*

A. TiO_2(B)

The structure of TiO_2(B) [2,3] can be describe as the association of ReO_3 [13] type TiO_2 chain which share corner along b axis and edge along a, c axes (figure 1.3).

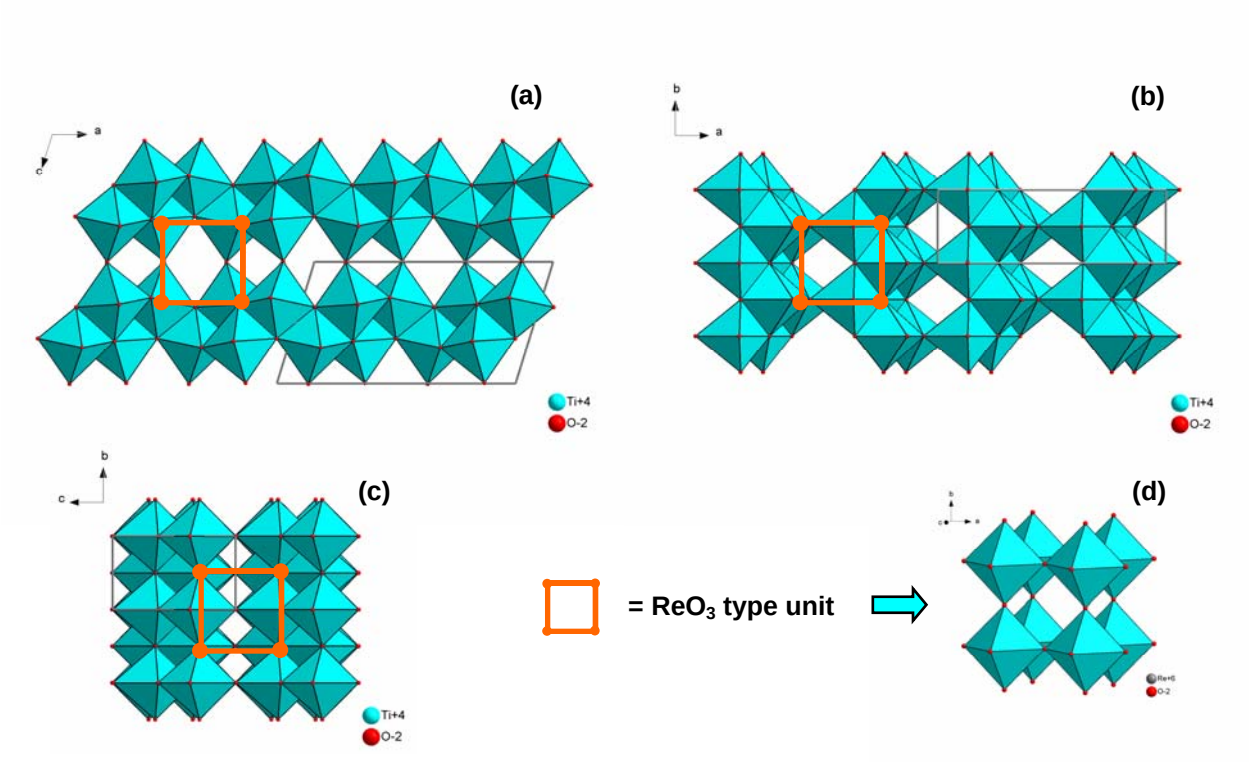

Figure 1.3. Structure of TiO_2(B): projection along (a) [010], (b) [001] and (c) [100]; (c) structure of ReO_3.

B. Anatase

We can regard anatase structure as a 3D combination of zigzag chains (along a or b axis) made up by TiO_6 octahedrons sharing their two adjacent edges with other two octahedrons. These zigzag chains along b axis (or a axis) combine with other chains by sharing the edge oxygen along a axis (or b axis) and c axis to form anatase structure (figure 1.4).

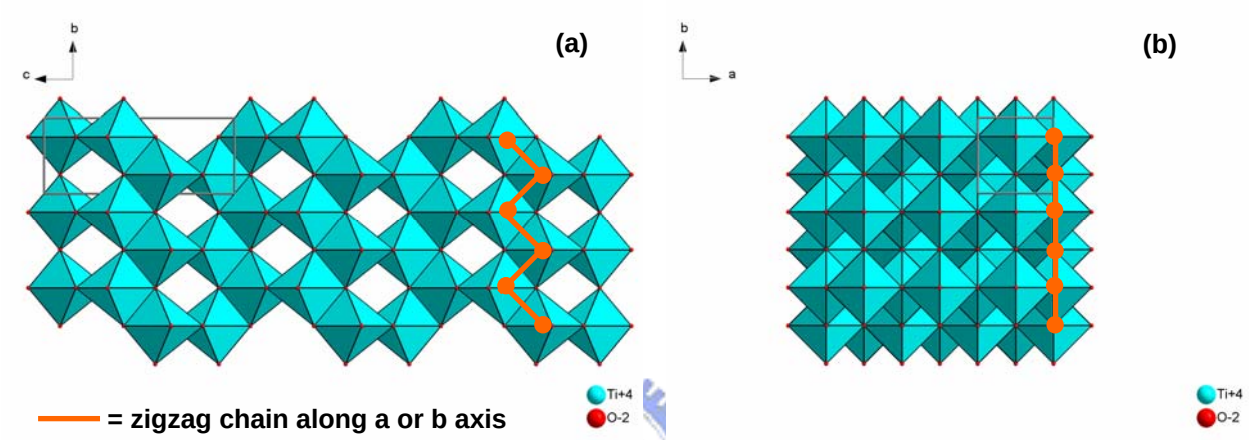

Figure 1.4. Structure of TiO_2 anatase: projection along (a) [100] and (b) [001].

C. Rutile

We describe rutile structure as a composition of TiO_2 chains, which are formed by TiO_6 octahedrons sharing their two parallel edges with other two octahedrons, by sharing their two opposite corner oxygen (figure 1.5). That forms a tunnel structure with square hole along c axis.

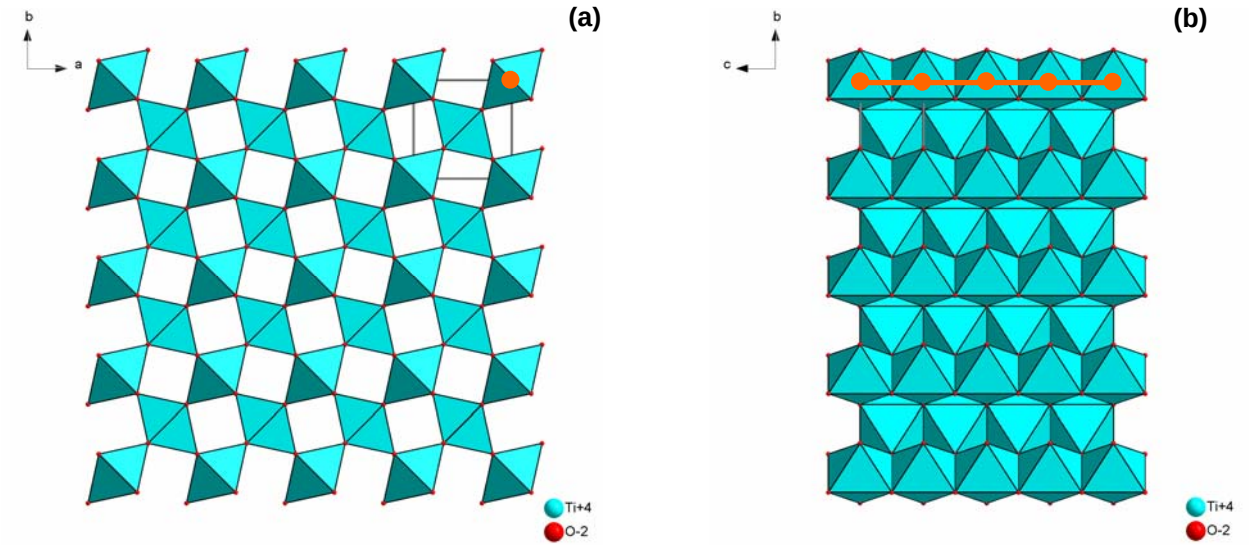

Figure 1.5. Structure of TiO_2 rutile: projection along (a) [001] and (b) [100].

D. Hollandite

The TiO_2 type hollandite is a more compact bonding structure of rutile one. It is constructed by a chain unit (along c axis direction) which is edge oxygen combination of double rutile chain units (marked by orange dashed ellipse in figure 1.6). This double unit associate with other four ones by sharing corner and edge oxygen to form a tunnel structure with two types of square hole along c.

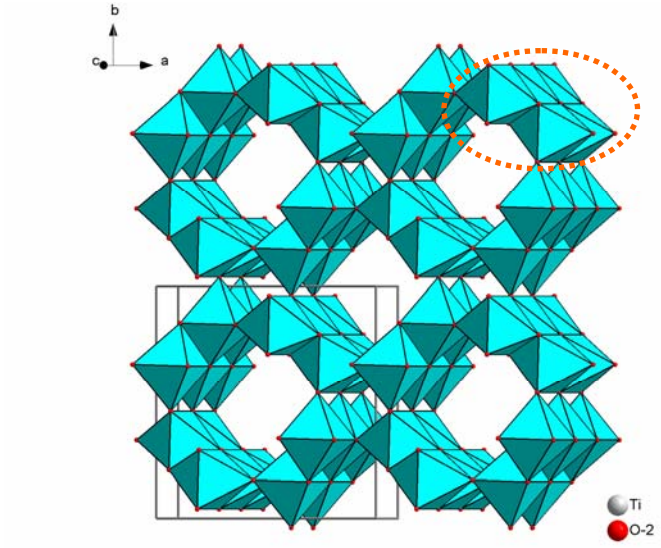

Figure 1.6. Projection along [1 0 10] of structural diagram of TiO_2 hollandite.

E. Ramsdellite

The ramsdellite type structure is an intermediate between rutile and hollandite. It is constructed by similar double chain unit (marked by orange dashed ellipse in figure 1.7) along c axis as hollandite one, but associated by sharing different corner and edge oxygen atoms with other four units to form a tunnel structure with rectangular hole along c.

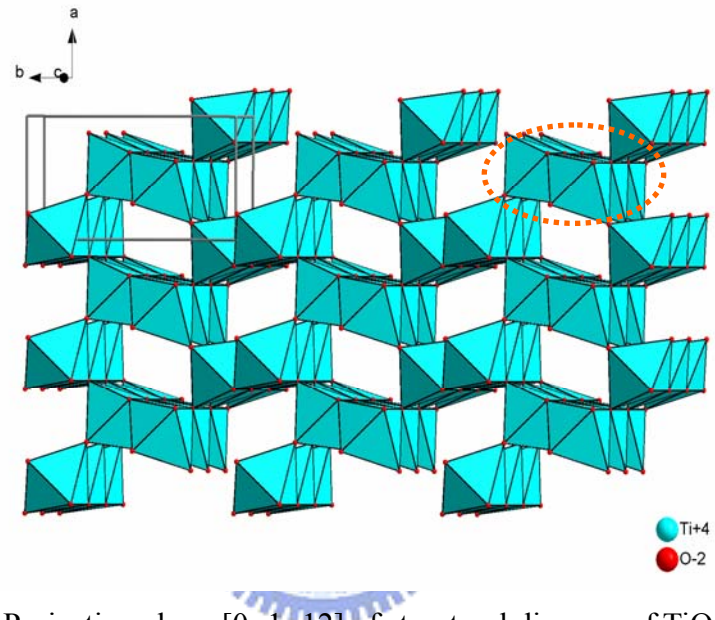

Figure 1.7. Projection along [0 -1 -12] of structural diagram of TiO_2 ramsdellite.

F. Brookite

The brookite structure can be described of an association of the zigzag chains along c axis (see figure 1.8) by sharing their corner oxygen with other four ones. This zigzag chain is constructed of TiO_6 octahedron connections by sharing the edges with other two ones.

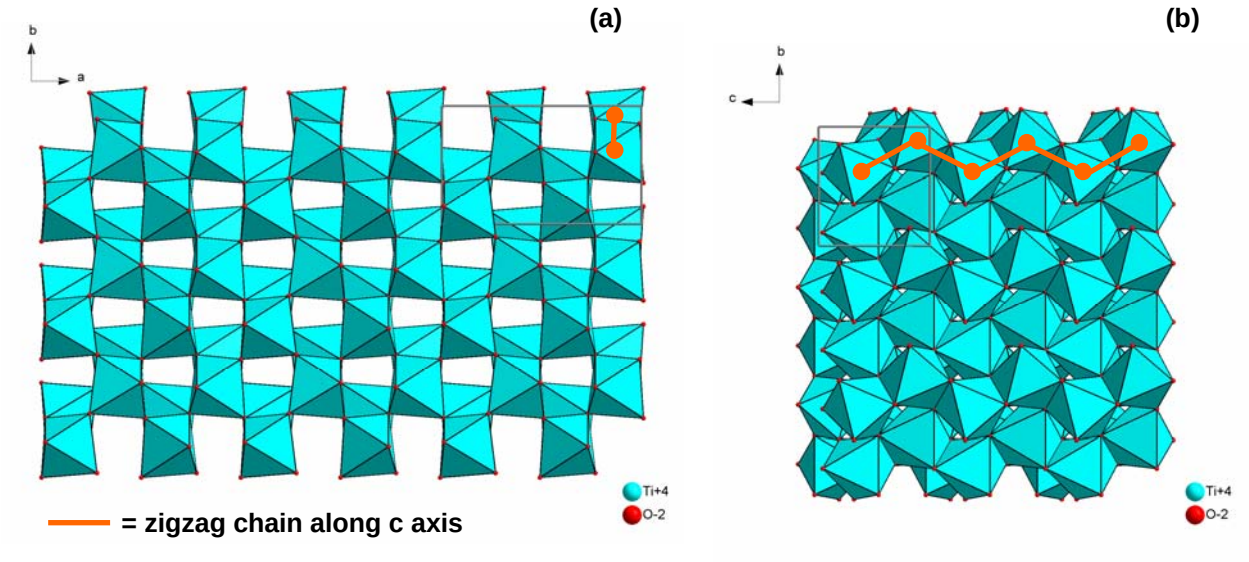

Figure 1.8. Structure of TiO_2 brookite: projection along (a) [001] and (b) [100].

G. TiO_2 type α-PbO_2 (TiO_2-II)

The TiO_2-II structure is constructed by the same zigzag chain unit along c axis with brookite, but different connection type with other units along a axis. We can describe the brookite one as "AABB" repeating mode and "ABAB" for the TiO_2-II one along a axis direction.

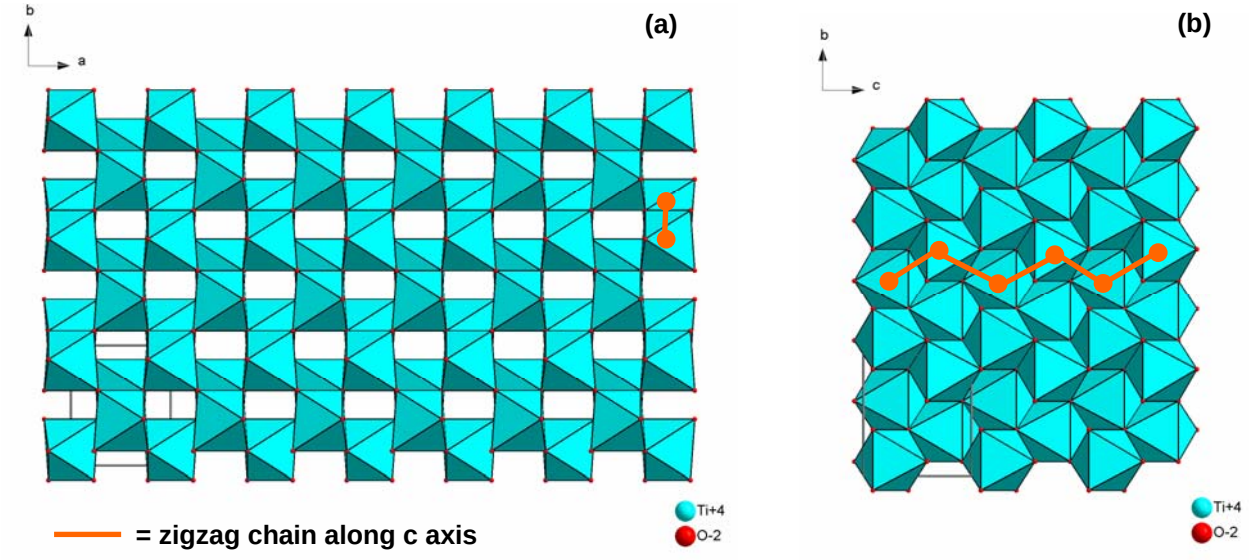

Figure 1.9. Structure of TiO_2-II: projection along (a) [001] and (b) [100].

H. Thermodynamics stability of various TiO_2 polymorphs

Thermodynamic calculations predict that rutile is the stablest phase at most of temperatures and pressures, but TiO_2(II) becomes the thermodynamic favourable phase up to 60 kbar.[14] Thermodynamic structure-based analyses confirm that the relative phase stability may reverse when particle sizes decrease to sufficiently low values due to surface free energy effects which depend on particle size.[15] If the particle sizes of the three nanocrystalline phases are equal, anatase is most thermodynamically stable at sizes less than 11 nm, brookite is most stable between 11 and 35 nm, and rutile is most stable at sizes greater than 35 nm.[16]

1.2.3. Properties and Applications of TiO_2

In the beginning of the 20th century, industrial production started replacing toxic lead oxides with titanium dioxide as pigments for white paint. Today, the world industrial production of TiO_2 exceeds 4 million tons.[17] It is used as a white pigment in paints (51%), plastic (19%), and paper (17%). The utilization of TiO_2 as a pigment increased in the last few years such as textiles, food, leather, pharmaceuticals (tablet coatings, toothpastes, and UV absorber in sunscreen cream and other cosmetic products).[1]

Recently, TiO_2 has received much attention to its chemical stability, non-toxicity, low cost, and other advantageous properties such as its high refractive index and dielectric constant (table 1.2).

Table 1.2. Some bulk properties of TiO_2 (anatase, brookite and rutile).[18,19]

	Density (g/cm^3)	Band gap (eV)	Reflective index		Dielectric property			
			n_g	n_p	Frequency (Hz)		Temperature (K)	Dielectric constant
anatase	3.83	3.2	2.57	2.66	(average)	10^4	298	55
brookite	4.17	3.4	2.81	2.68	-	-	-	-
					(perpendicular to optical axis)	10^8	290-295	86
					(parallel to optical axis)	10^8	290-295	170
rutile	4.24	3.0	2.95	2.65	(perpendicular to c axis)	10^4	298	160
					(parallel to c axis)	10^7	303	100

As a result of its high refractive index, it is used as anti-reflection coating in silicon solar cells and in many thin-film optical devices.[20] Due to the high dielectric constant of rutile (e > 100), it is investigated as a dielectric gate material for MOSFET devices.[21] Moreover, the doped anatase films with Co might be used as a ferromagnetic material in spintronics.[22] TiO_2 is also successfully used as gas sensor due to the dependence of the electric conductivity on the ambient gas composition such as in the determination of CO/O_2, CO/CH_4 concentrations.[23] Due to its compatibility with the human body, TiO_2 is used as a biomaterial such as bone substituent and reinforcing mechanical supports.[24] In lithium ion batteries, the anatase and TiO_2(B) form is used as an anode material in lithium ion intercalation reversibly.[25-27]

1.2.4. Photoinduced processes and applications of TiO_2 [1]

Today, the hottest field of TiO_2 is its photoinduced phenomena (figure 1.2). All these photoinduced processes originate from the semiconductor band gap of TiO_2. When incentive photons have a higher energy than the band gap, they can be absorbed and electrons are

promoted to the conductive band, leaving a hole in the valance band. This excited electron can either be used to create electricity (photovoltaics)[28] or drive a chemical reaction (photocatalysis).[29] A special phenomenon called "photoinduced superhydrophilicity" was recently discovered. It originates from trapping of photoinduced holes on the TiO_2 surface causes a super hydrophilicity.[30] All photoinduced phenomena involve surface bound redox reactions represent as following equations and figure 1.10:

$$(Ox)_{ads} + (Red)_{ads} \xrightarrow[TiO_2]{h\nu} (Ox^-)_{ads} + (Red^+)_{ads}$$

(Detail example)

$$TiO_2 + h\nu \rightarrow TiO_2\ (e^-, h^+)$$

$$TiO_2\ (h^+) + RX_{ads} \rightarrow TiO_2 + RX_{ads}^{\bullet +}$$

$$TiO_2\ (h^+) + H_2O_{ads} \rightarrow TiO_2 + OH_{ads}^{\bullet} + H^+$$

$$TiO_2\ (e^-) + RX'_{ads} \rightarrow TiO_2 + RX'^{\bullet -}_{ads}$$

$$TiO_2\ (e^-) + O_{2,ads} \rightarrow TiO_2 + O_2^{\bullet -}$$

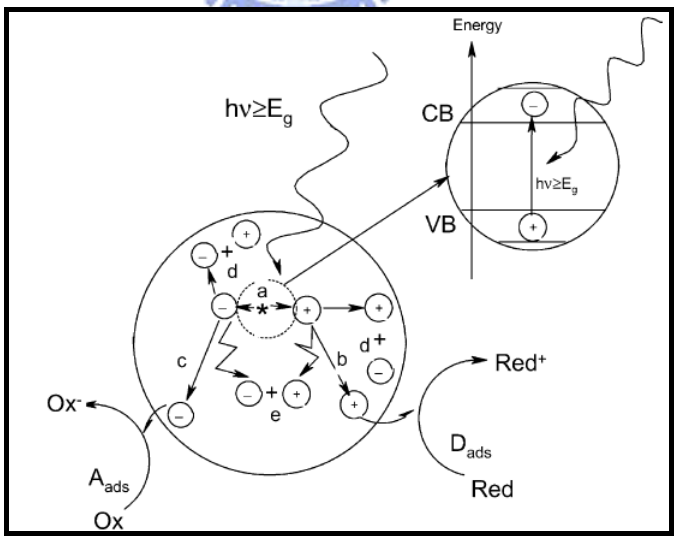

Figure 1.10. Photoinduced process on semiconductor: (a) electron–hole generation; (b) oxidation of donor (D); (c) reduction of acceptor (A); (d) and (e) electron–hole recombination at surface and in bulk, respectively.[1]

We can apply the property above to the photodegeneration of organic compounds. TiO_2 is a photocatalyst in environmental decontamination for a large variety of organics,[31] viruses, bacteria,[32] fungi, algae, and cancer cells[33] totally degraded to CO_2, H_2O, and harmless inorganic anions. By the same working principle, photosynthesis,[34] photoreduction,[34] photoelectrolyse[29] and photoinduced superhydrophilicity[30] can be carried out.

Some imortant development of TiO_2 in photoactivated processes are:

1972 Fujishima and Honda, the first photoelectrochemical cell for water splitting ($2H_2O \rightarrow 2H_2 + O_2$).[29]

1977 Frank and Bard reported the reduction of CN^- in water, the first implication of TiO_2 in environmental purification.[31]

1977 Schrauzer and Guth reported the photocatalytic reduction of molecular nitrogen to ammonia ($2N_2 + 6H_2O \rightarrow 4NH_3 + 3O_2$) over iron-doped TiO_2.[34]

1985 T. Matsunaga, R. Tomato, T. Nakajima and H. Wake applied TiO_2 to photokill Lactobacillus acidophilus, Saccharomyces cerevisiae and Escherichia coli.[32]

1991 O'Regan and Grätzel reported an efficient solar cell using nanosized TiO_2 particles.[28]

1998 Wang et al. reported highly hydrophilic TiO_2 surfaces with excellent self-cleaning properties.

1.2.5. Improving the photoactive efficiency of TiO_2

Common TiO_2 has photonic efficiency of less than 10% for most photoinduced process. Improving the photocatalytic performance is an important topic for TiO_2. The high performance of a good photocatalyst is related simultaneously (i) to a good capacity of adsorbing reactants and (ii) to a good ability of absorbing photons to create photoinduced electrical charges.[35] In other words, the photoactive efficiency is not necessarily depending on surface area but rather on the availability of active site. Therefore, although *small particle size*[36] and *large surface area*[37] are the acknowledged elementary properties for improving photocatalytic ability, other properties as *crystalline structure*, *pore size*, *OH group density*, *surface acidity*, *number and nature of trap site* and *adsorption/desorption characteristics* also play an very important role in photocatalytic efficiency.[1]

Except the properties mentioned above, *doping* and *metal coating* are very important artifices to enhance the performance.[36] Moreover, *hybrid with other semiconductor*[38] and *dye sensitization*[28] are also good method to modify the properties of TiO2.

1.2.6. Synthesis of TiO_2

A. Industrial mass production process

In industrial mass production, titanium dioxide may be manufactured by the sulfate or the chlorine process.[39] In the sulfate process, ilmenite is transformed into iron- and titanium sulfates by reaction with sulfuric acid. Titanium hydroxide is precipitated by hydrolysis, filtered, and calcinated at 900° C. Straight hydrolysis yields only anatase on calcination. The alkakine hydrolysis is necessary to obtain rutile.

The chlorine process uses crude qulity rutile which is produced from ilmenite using the Becher process. The Becher process heats the ilmenite with coal and sulfur to reduce the iron

oxide in the ilmenite to metallic iron and then reoxidizes them to separate out the titanium dioxide as rutile about 90% purity. The rutile is reacted with recycled chlorine to produce titanium tetrachloride, and then reoxidized yielding very pure TiO_2.

B. In gas phase

Most thin film synthesis are performed from gas phase method, such as chemical vapor deposition (CVD) by chemical reaction or decomposition of precursor in gas phase[40]; physical vapor deposition (PVD) without chemical reaction of precursor[41]; and spray pyrolysis deposition (SPD) from pyrolysis of aerosol precursor on substrate.[42]

C. In solution phase

In laboratory, to prepare TiO_2 as powder or thin film form, especially as nanocrystalline, liquid phase process is the most convenient method. They involve precipitation methods,[43] solvothermal methods,[44] sol-gel methods,[45] microemulsion methods,[46] combustion methods[47] and electrochemical synthesis.[48]

D. Condensation mechanism of TiO_2 in solution reaction[49]

Since about 20 years ago, chimie douce (solvothermal) method has developed on synthesis of TiO_2 and titanate with organic or inorganic cation. We call this method as "douce" because of the mild temperature condition from ambient to 300° C. Under this mild reaction condition, synthesis of metastable phase product and structural control, such as tunable size, morphology, structure etc. become possible. The comprehension of polycondensation mechanism of metal polycation is very important to handle the synthetic parameters.

In J. P. Jolivet's writings, "*de la solution a l'oxyde*",[49] he compiled and explained the condensation mechanisms of metal oxides precipitation at aqueous solution in plain diagrams.

We extracted some paragraphs to introduce the condensation of TiO_2 in aqueous solution.

In condensation processes, we can describe as three stages: initiation (hydroxylation), propagation (olation) and termination (oxolation) (see figure 1.12). In initiation (hydroxylation), the hydroxo ligands were created in coordination sphere of precursor by directly bonding or replacing some original ligands on metal ion. The type of hydroxo ligand depends on cation charge and pH of solution (figure 1.11).

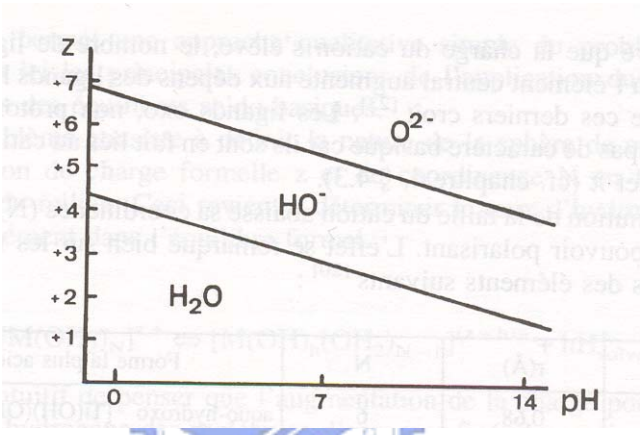

Figure 1.11. Diagram represents the nature of ligands on a coordinated cation with ion charge z and environmental pH.[49]

At aqua zone (H_2O), water coordinates as legand, and there is no more H on legand in oxo zone. We can express the formation of hydroxo ligand on precursor monomer with H^+ or OH^- as:

$$[M\text{-}O]^- + H_3O^+ \leftrightarrow [M\text{-}OH] + H_2O \leftrightarrow [M\text{-}OH_2]^+ + OH^-$$

In propagation (olation and oxolation) (figure 1.12), the above hydroxo cation monomers condense assembly by formation of bridging (sharing) oxygen between two or more cations. We can represent the olation process as following equation:

$$\text{-M-OH} + \text{-M-OH}_2 \rightarrow \text{-M-OH-M-} + H_2O \qquad \text{(olation)}$$

If there is no more aqua legand in the coordination sphere, the oxolation will be proceeded:

$$\text{-M-OH + -M-OH} \rightarrow \text{-M-O-M- + } H_2O \qquad \text{(oxolation)}$$

A succession of hydroxolation, topotatic olation and oxolation constitute the polycondensation of metal oxide in aqueous solution until precipitation formed. The termination point depends on the thermodynamics of reaction, related to nature of precursor, concentration, pH, temperature, duration…etc. In figure 1.12, we can observe the influence of intermediate species form to final product.

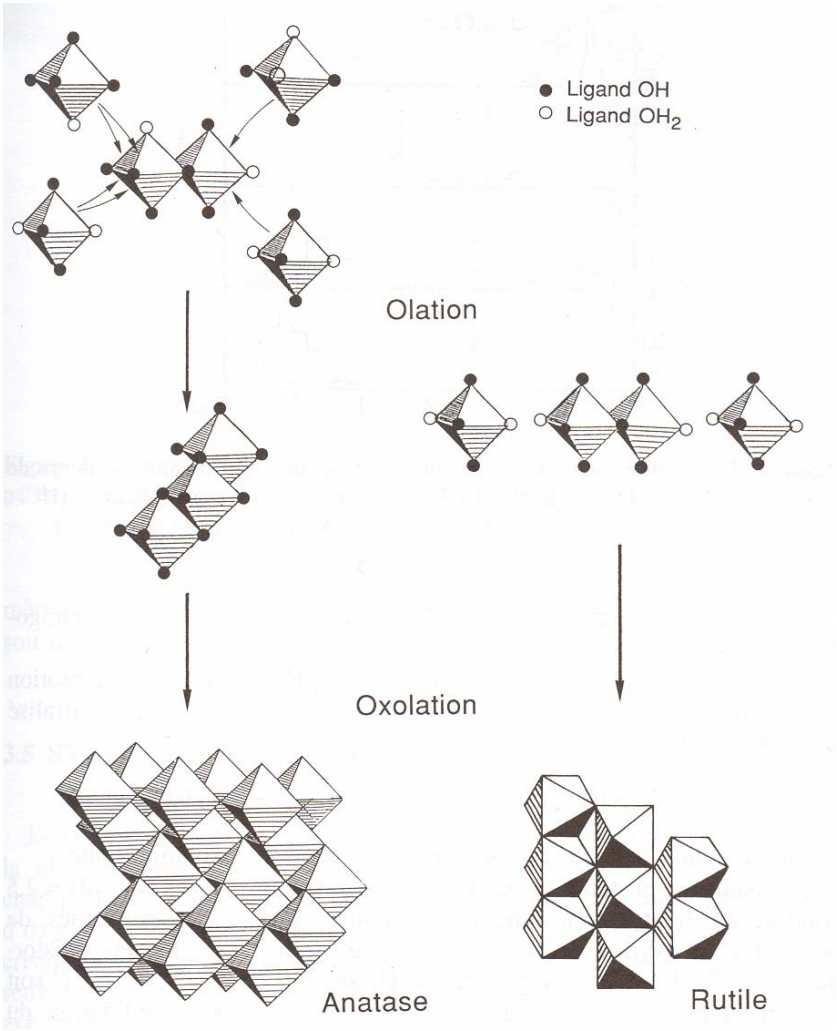

Figure 1.12. Possible reaction routes of the formation of rutile and anatase phase TiO_2 from aqueous solution.[49]

1.3. Synthesis and Structure of Alkali Titanates

The alkali titanate structure has been presented since 1960s by S. Anderson and A. D. Wadsley.[50,51] Their synthetic and structural studies are investigated continually until now. They have fibrillar form and excellent ion exchange ability. They can be expressed as a general formula "$M_2Ti_nO_{2n+1}$" owning layer structure ($3 \leq n \leq 5$) or tunnel structure ($6 \leq n \leq 8$), the alkali M occupied in the interlayer or tunnel space. Generally, they are synthesized from calcinations of TiO_2 and alkali salt (such as alkali carbonate or nitrate) mixture at 800-1000° C in air during several hours to days.

The titanate layers are constructed starting from the indentical chains of n distorted TiO_6 octahedrons join each other by sharing edge. These octahedral chains assemble together as zigzag by connecting corner along c axis and edge along b. The layers are isolated in the structures with composition $3 \leq n \leq 5$ (see figure 1.13 and table 1.3) and condensed by sharing corner to form tunnel structure with composition $6 \leq n \leq 8$ (figure 1.14).

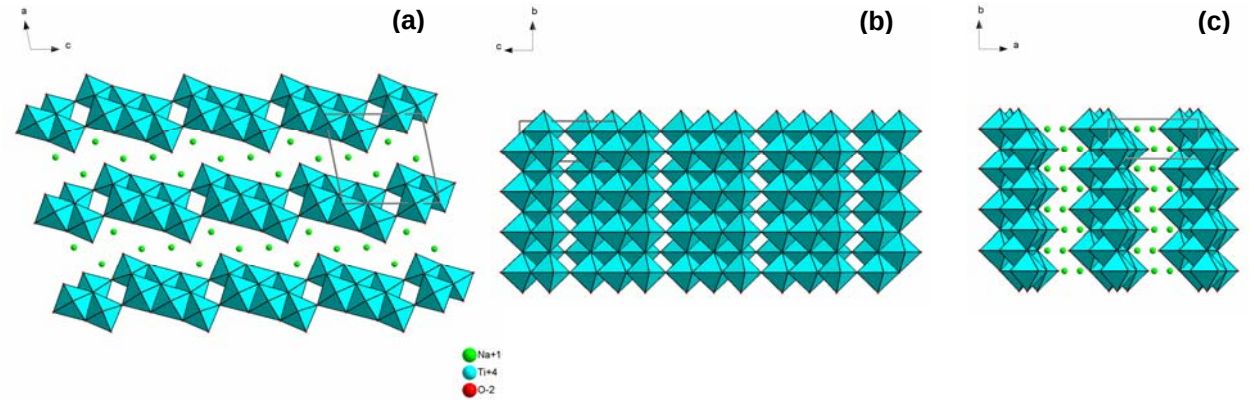

Figure 1.13. Structural diagram of sodium trititanate $Na_2Ti_3O_7$ (layer structure, n=3) viewing along (a) [010], (b) [100] and (c) [001].[50]

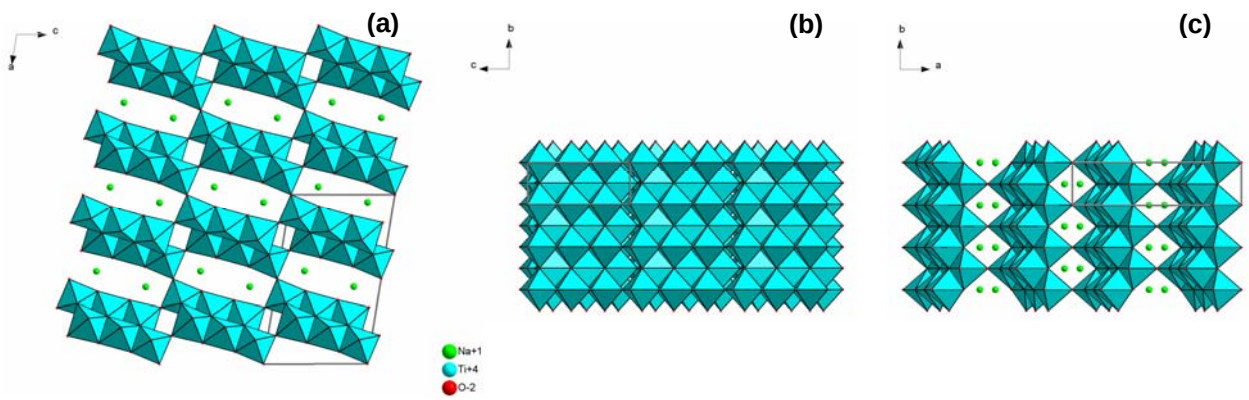

Figure 1.14. Structural diagram of sodium hexatitanate $Na_2Ti_6O_{13}$ (tunnel structure, n=6) viewing along (a) [010], (b) [100] and (c) [001].[50]

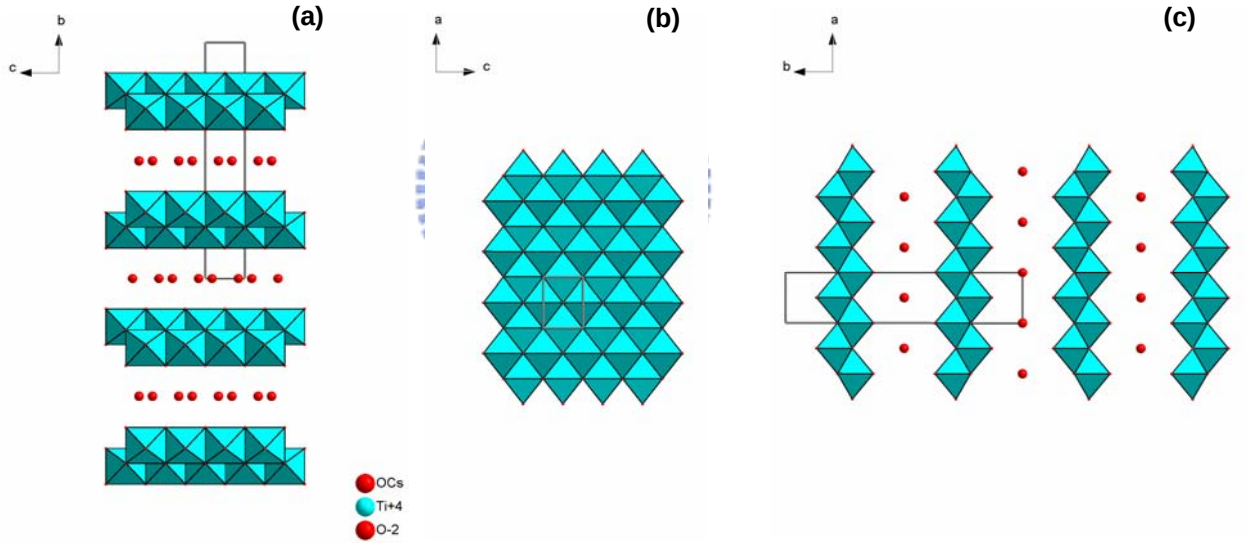

Figure 1.15. Structural diagram of cesium hexatitanate $Cs_2Ti_6O_{13}$ (lepidocrocite, γ-FeO(OH), type layer structure, n=∞) viewing along (a) [100], (b) [010] and (c) [001].[53]

The lepidocrocite (γ-FeO(OH)) type layer structure ($Cs_2Ti_6O_{13}$ in table 1.3) is distinctive, its number of octahedrons is infinitive (n=∞). The octahedral chain along c axis does not present as zigzag form, so that the system is not monoclinic (β≠90°) as others but orthorhombic.

On space group, we can differentiate them as primitive (P) or c-center (C) due to the

layer (as zigzag chain viewing along c) is identical or opposite with adjacent layers (see figure 1.16) along b axis.

Table 1.3. Various alkali titanate structures: number of octahedrons repeating along c and lattice parameter.[104-106]

composition	number of octaherons	a (Å)	b (Å)	c (Å)	β(°)	V (Å^3)	Z	space group	ref.
γ-FeO(OH)	∞	3.06(2)	12.51(1)	3.87(1)		148.1(8)	4	*Cmcm*	52
$Cs_2Ti_6O_{13}$	∞	3.825(2)	17.271(7)	2.961(1)		195.60(1)		*Immm*	53
$Cs_2Ti_5O_{11}$	5	19.718(8)	3.808(1)	15.023(6)	106.93(3)	1079.1(1)	4	*C2/m*	54
$K_2Ti_4O_9$	4	18.17(1)	3.789(6)	12.025(6)	106.30(4)	797.1(1)	4	*C2/m*	55
$Tl_2Ti_4O_9$	4	18.98(3)	3.78(5)	12.05(3)	106.8(2)	826.8(1)	4	*C2/m*	56
$Na_2Ti_3O_7$	3	8.571(2)	3.804(2)	9.135(2)	101.57(5)	236.6(1)	2	*P2/m*	50
$K_3Ti_8O_{17}$	4*	15.68(1)	3.809(2)	12.06(1)	95	717.5	2	*C2/m*	57
$K_2Ti_8O_{17}$	4*	15.62(2)	3.771(2)	11.93(3)	95.8(3)	699.1	2	*C2/m*	58
$Na_2Ti_7O_{15}$	4-3*	14.9(1)	3.74(1)	20.9(1)	96.5(5)	1157.2(1)	4	*C2/m*	59
$K_2Ti_6O_{13}$	3*	15.593(3)	3.796(1)	9.108(1)	99.78(1)	531.28(1)	2	*C2/m*	60
$Ba_2Ti_6O_{13}$	3*	15.004	3.953	9.085	98.01	533.58	2	*C2/m*	61
$Na_2Ti_6O_{13}$	3*	15.131(2)	3.745(2)	9.159(2)	99.30(5)	512.2(1)	2	*C2/m*	50
$Rb_2Ti_6O_{13}$	3*	15.89	3.82	9.11	100.4	543.9	2	*C2/m*	62
$K_2SrTi_{10}O_{22}$	3-2*	15.314(2)	3.7865(6)	15.439(2)	102.68(1)	873.42(4)	2	*C2/m*	63

* Tunnel structure.

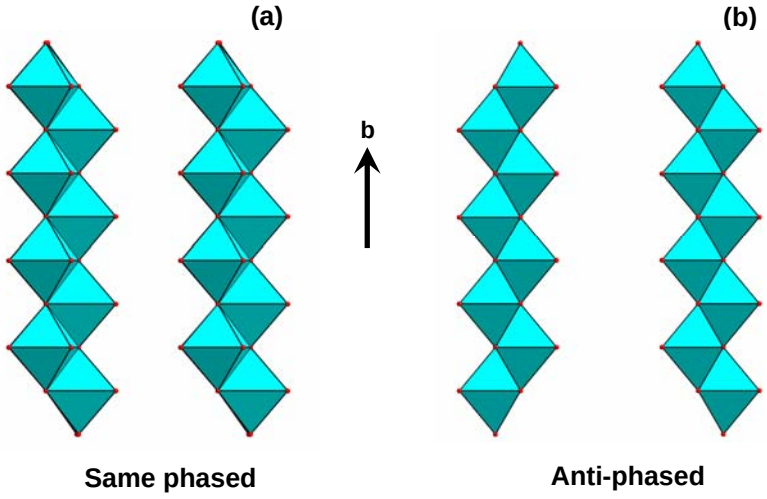

Figure 1.16. Phased (primitive, P) and anti-phased (c-center, C) titante layer structures.[105,106]

1.4. Synthesis and Applications of Titanate Nanostructures

1.4.1. Review of synthesis of titanate nanostructure

The hydrothermal method has been employed to synthesize titante from TiO_2 and NaOH at the reaction temperaure lower than solid state method (800-1000° C) since later half of 1960s.[64,65] Even though that, their operation temperature is still high (350-600° C). In 1981, M. Wanabe investigated the diagram Na_2O-TiO_2 on hydrothermal condition at 250-550° C.[66] They all focused on milder synthetic condition of titanate. The results reveal hydrothermal reaction indeed make Na ion possible to attack TiO_2 at temperature much lower than 800° C.

Since the unique graphene based nanostructure, carbon nanotube (CNT), was discovered by S. Iijima in 1991,[67] the studies of nanostructures started to make a great leap. The other tubular nanostructures as BN nanotube[68] and surfactant intercalated VO_x nanotube[69] were synthesized following. By another route, ceramic nanotubes such as SiO_2, Al_2O_3, V_2O_5, and MoO_3, have been prepared by template method.[70]

In 1998, T. Kasuga et al. first synthesized titania nanotube from fine anatase TiO_2 powder in 10M aqueous NaOH solution at 110° C. The TiO_2 nanotubes with a diameter of 8 nm and a length of 100 nm have a large specific surface area about 400 m^2g^{-1}.[71,72] In 2002, L. M. Peng et al. repeated T. Kasuga's experiment, first observed the nanotube roll up by single titanate layer and proposed a possible trititanate based rolling structure (see figure 1.17).[73,74]

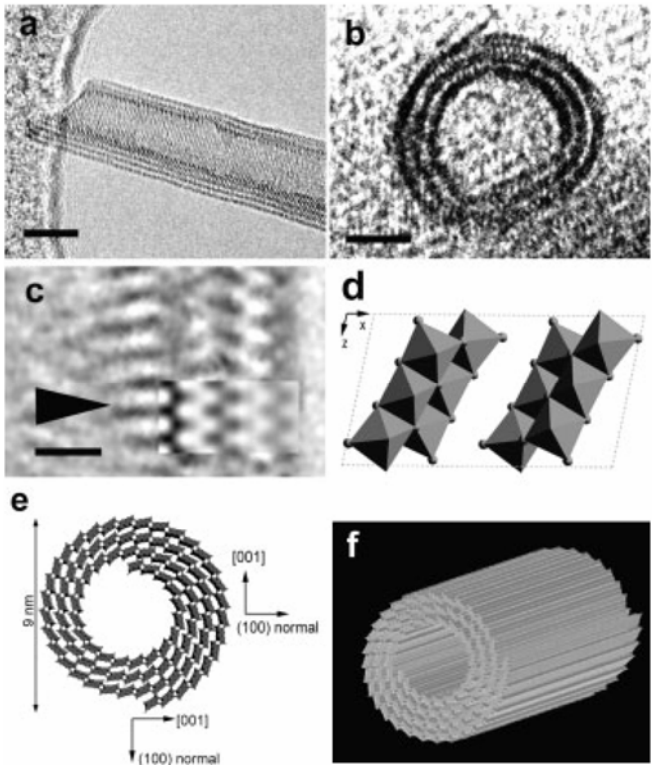

Figure 1.17. (a) side view and (b) top view of an open-end titanate nanotube; (c) HRTEM and simulation image of the wall part of (a); (d) diagram of a unit cell of $Na_2Ti_3O_7$ along [010]; (e) diagram of $Na_2Ti_3O_7$ nanotube rolling structure along [010]; (f) 3D view of $Na_2Ti_3O_7$ nanotube.[73]

However, the disputations of the real structure titante nanotube have never ended. The results about the growth mechanism and structure of titanate nanotube have been reported constantly.[75-82] They proposed various tiania or titanate structure involve $Na_2Ti_3O_7$ (figure 1.17)[73], anatase (figure 1.18 and 1.19)[75,76,79], $Na_2Ti_2O_4(OH)_2$ (figure 1.20)[78], Na_2TiO_3 (figure 1.21)[80] and lepidocrocite (figure 1.22)[77,82] to explain the growth mechanism.

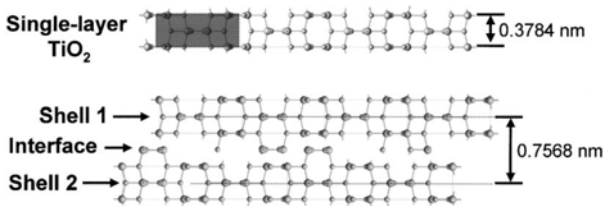

Figure 1.18. Schematic drawing of an anatase single layer and the tube wall structure formed by the single-layer sheets. Shadowed area indicates the unit cell of the anatase phase.[76]

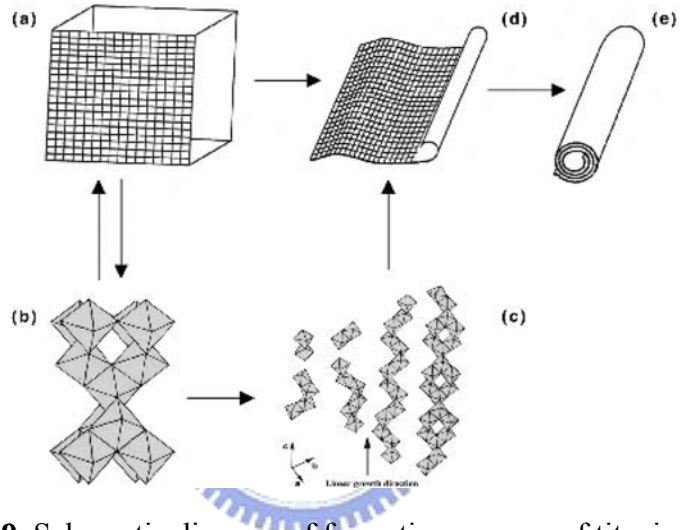

Figure 1.19. Schematic diagram of formation process of titania nanotube.[79]

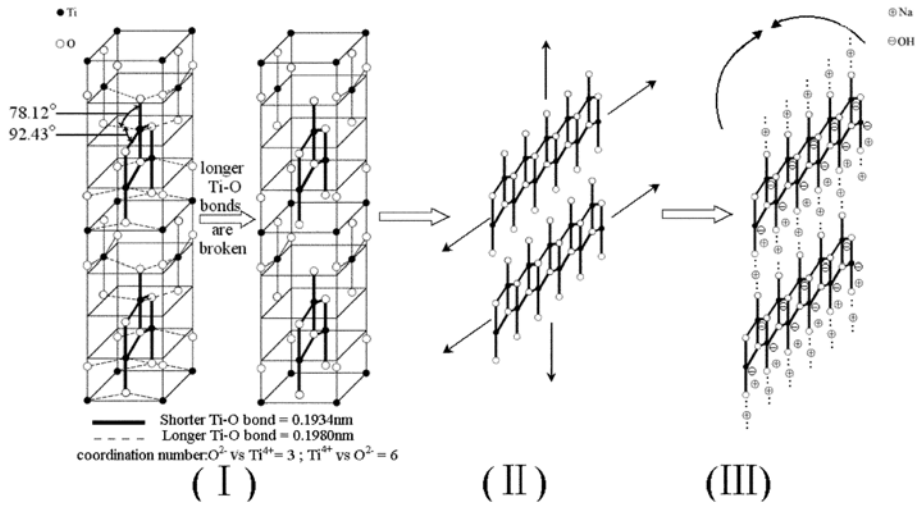

Figure 1.20. Schematic diagram of formation process for nanotube $Na_2Ti_2O_4(OH)_2$.[78]

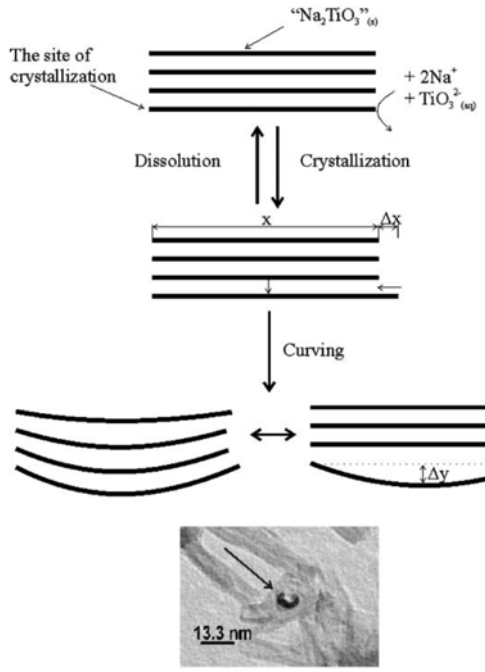

Figure 1.21. Schematic diagram showing proposed transformation of multilayered nanosheets to nanotubes.[80]

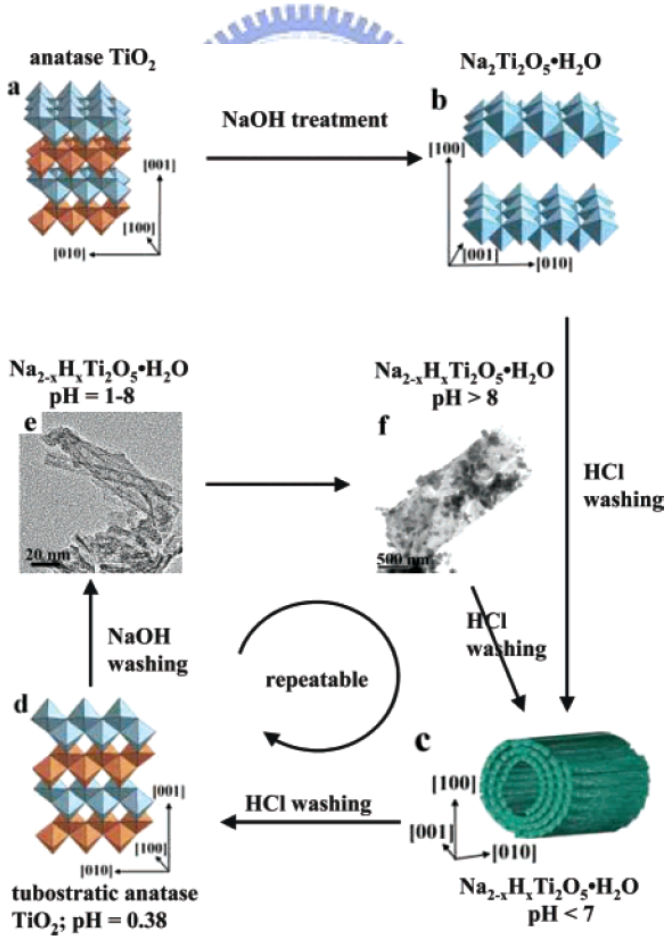

Figure 1.22. Overall scheme for the formation and transformation of nanotubes induced by the NaOH treatment and the post-treatment washing.[82]

On the other side, there is not only tubular phase being observed, but also nanosheet (figure 1.23)[83], nanofiber (figure 1.24)[84] and nanowire (figure 1.25)[85,86] existed in similar process. The sheet-like titante product was obtained in lower basic concentration (5M $NaOH_{(aq)}$).[83] The nanofiber was synthesized from amorphous TiO_2 gel.[84] And the nanowire was observed in higher temperature condition (180° C -200° C). [85,86] Therefore, we can infer that the morphologic control parameters at least involve basic concentration, structure of precursor, and reaction temperature.

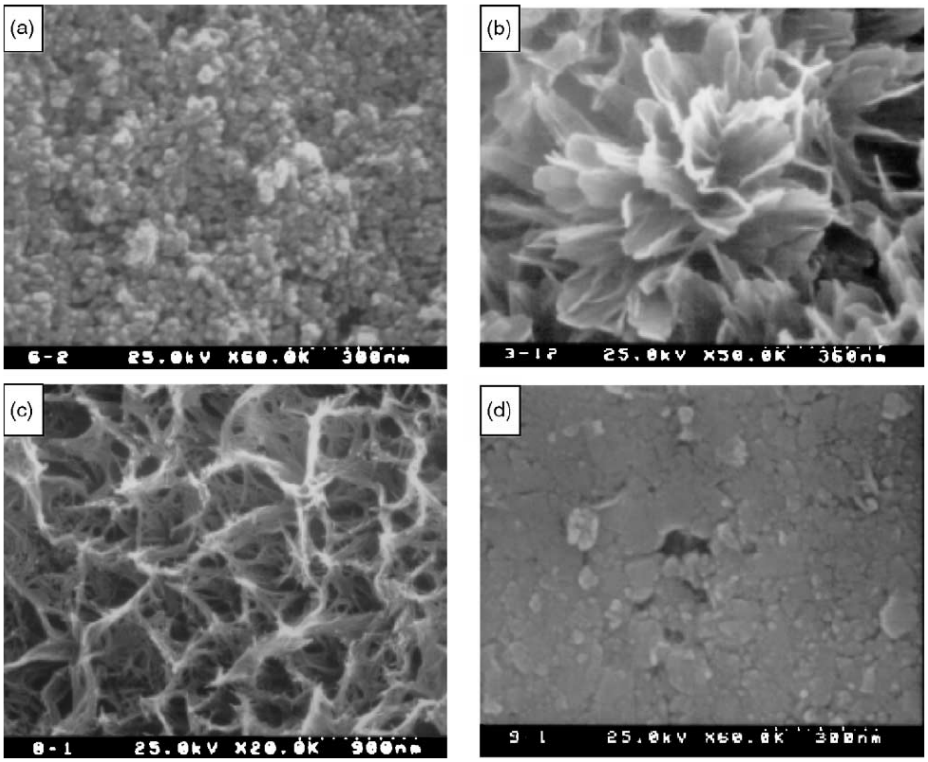

Figure 1.23. SEM images for: (a) raw materials (calcined at 673 K), (b) treated by 5M NaOH, (c) treated by 10M NaOH, and (d) calcined at 1173K followed by 10M NaOH at 423K for 20 h.[83]

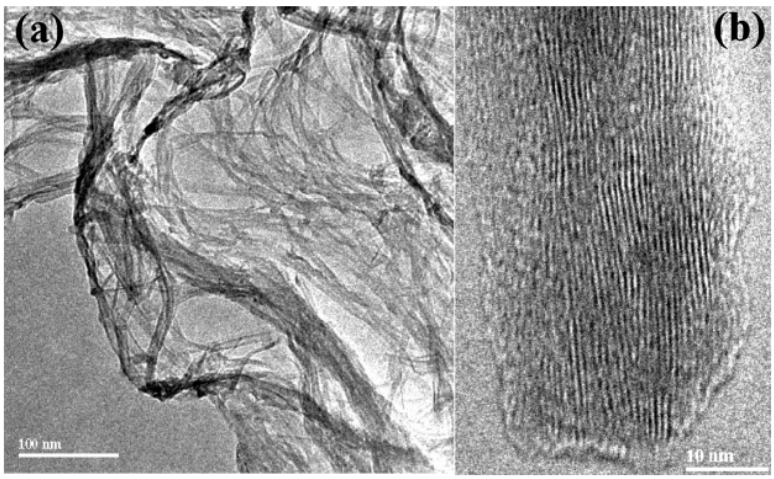

Figure 1.24. (a) Low-magnification TEM image of titanium oxide nanomaterials, showing well-interlinked structure; (b) HRTEM image of a nanofiber, revealing the layered structure.[84]

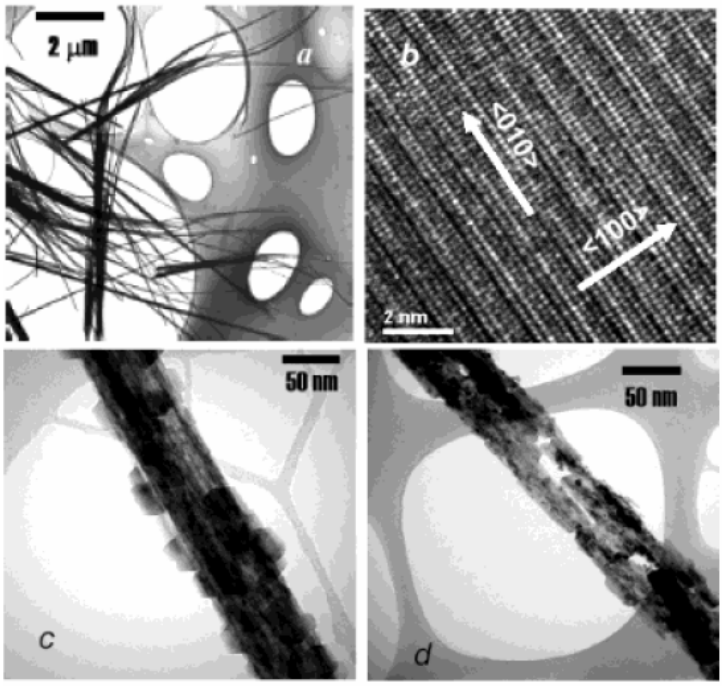

Figure 1.25. TEM images of the samples. (a) H-titanate wires, (b) HRTEM image of the wires, (c) the product of the phase conversion reaction at 373 K and (d) the product obtained at 393 K.[86]

1.4.2. Applications of titanate nanostructure

The nanostructures of alkali hydroxo titanate have two advantaged properties for

application: (i) very large specific surface (200-400 m^2g^{-1})[87]; (ii) excellent ion exchange ability.(cation exchangeable in solution)[88] The further one reveals potential of surface property related applications, and the second one implies that we can easily modify their structure and properties by replacing cation[89] or coating/doping metal.[90]

There have been many properties and applications of titanate nanotubes tested and reported, such as *lithium intercalation* (figure 1.26),[91-93] *photocatalysis*,[94-97] *solar cell*,[98] *hydrogen storage*[99,100] and *photoluminescence*[101].

Except for hydrogen storage, all other test of property exhibits that the pretreated (ion-exchanged, doped, annealed…etc.) nanotube has better property. For lithium intercalation, TiO_2(B) phase after calcinations reveals better reversibility than raw product.[91-93] In photocatalyse, the N-doped,[95] Au-doped[96] and CdS hybrid[97] one exhibit good photoactivity, but nanotube without doping is inactive.[94] In solar cell case also reveals the CdS-doping nanotube has good photovoltaic ability.[98]

There are not many data about the properties and applications of nanosheet and nanowire product. We have already known the TiO_2(B) nanowire is good candidate for lithium intercalation.[93]

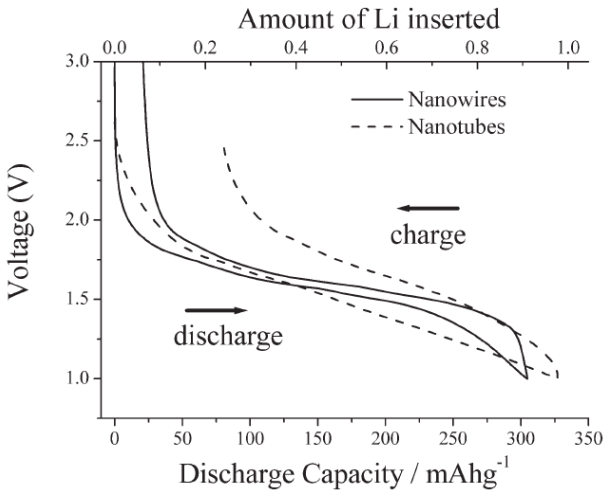

Figure 1.26. Variation of potential, vs. Li/Li^+ (1 M) electrode, with Li content (charge passed) for TiO_2-B nanotubes and nanowires cycled.[93]

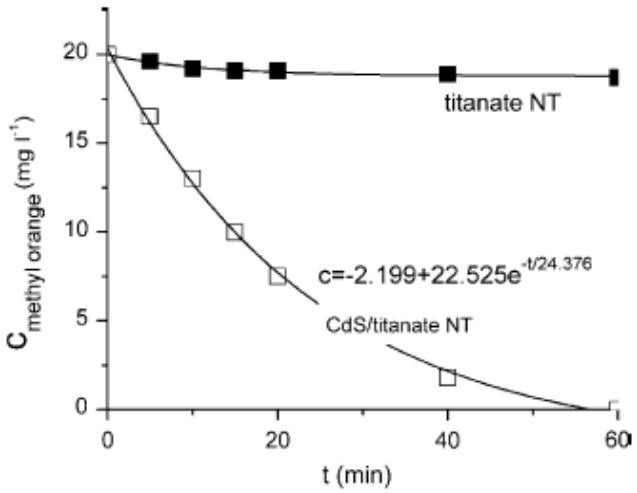

Figure 1.27. Photocatalytic activity of pristine trititanate nanotubes (solid squares) and CdS doped trititanate nanotubes (open squares).[97]

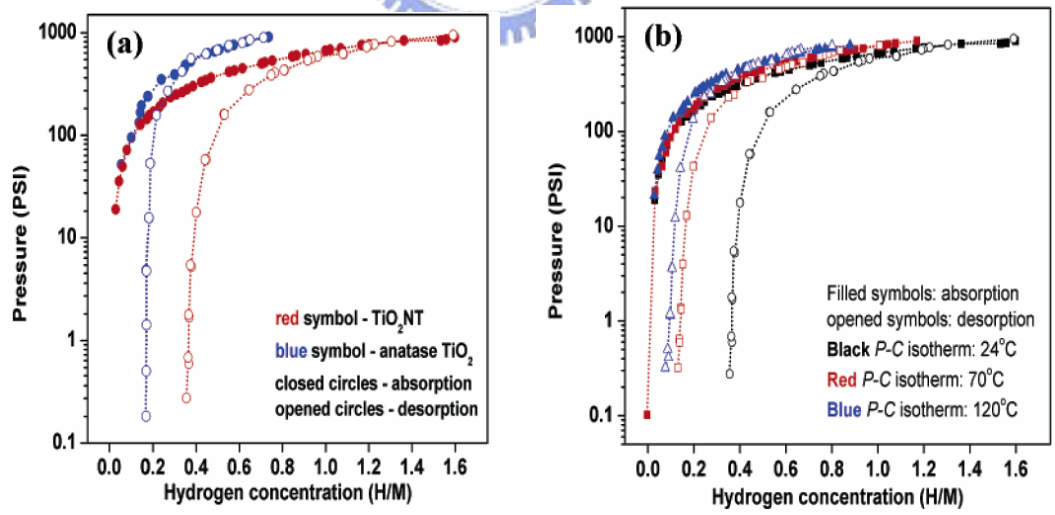

Figure 1.28. (a) *P-C* isotherms of TiO_2 nanotubes and bulk TiO2 at room temperature. (b) *P-C* isotherms of TiO_2 nanotubes at 24, 70, and 120 °C.[100]

1.5. Conclutions

Today, environmental protections and search renewable energy sources have been two global critical problems. Titanium oxides and titanates are regarded as powerful candidates as solar energy application materials due to their non toxic, low cost, abundance, good photo-electric-chemical properties and multi-functional applications. However, the photocatalytic efficiency is still improvable. In order to increase the photocatalysis performance, we need to modify the material structure, to enhance reactant adsorbability and effective photon absorbability. The nanostructuration of TiO_2 is a direct route to achieve these goals.

The chimie douce method provides a controllable artifice by gradual polycondensation of titanium hydroxo initiator. To employ this method, alkali titanate nanostructures were obtained from aqueous basic solution at much milder temperature (100 º C -200º C) than traditional solid state synthesis (800 º C-1000 º C). These nanomaterials were verified having large specific surface area (200-400 m^2g^{-1}) and good photo-electro-chemical properties after appropriate modification (ion exchange, annealing, doping…etc.). Although the structure has not been decided yet, the titanate nanotubes were reported to find applications in lithium intercalation, photocatalysis, solar cell and hydrogen storage.

In this thesis, we try to tune the reaction conditions such as the nature of precursors, basic or sodium concentration, temperature and carbonate concentration. Then we observe the change of product structure and morphology to discuss the correlations between conditions and products. We also studied these obtained structures for further comprehension of growth mechanism. In the last, we have measured their photoactivity and ability to lithium intercalation for possible applications. Our objective is to make tunable and applicable titanate nanostructures.

1.6. Reference

[1] O. Carp, C.L. Huisman and A. Reller, *Progress in Solid State Chemistry* **2004**, *32*, 33–177.

[2] R. Marchand, L. Brohan and M. Tournoux, *Mat. Res. Bull.* **1980**, *15*, 1129.

[3] T. P. Feist and O. K. Davis, *J. Solid State Chem.* **1992**, *101*, 275.

[4] JCPDS, ref.21-1272, *Nat. Bur. Stand. (US) Monogr.* **1969**, *25*.

[5] T. E. Weirich, M. Winterer, S. Seifried, H. Hahn and H. Fuess, *Ultramicroscopy* **2000**, *81*, 263.

[6] J. K. Burdett, T. Hughbanks, G. J. Miller, J. W. Richardson, and J. V. Smith, *J. of the Am. Chem. Soc.* **1987**, *109*, 3639-3646.

[7] R. J. Swope, J. R. Smith and A. C. Larson, *American Mineralogist* **1995**, *80*, 448.

[8] M. Latroche, L. Brohan, R. Marchand and M. Tournoux, *J. of Solid State Chem.***1989**, *81*, 78-82.

[9] J. Akimoto, Y. Gotoh, Y. Oosawa, N. Nonose, T. Kumagai, K. Aoki and H. Takei, *J. of Solid State Chem.* **1994**, *113*, 27-36.

[10] E. P. Meagher and G. A. Lager, *Canadian Mineralogist* **1979**, *17*, 77-85.

[11] P.Y. Simons and F. Dachille, *Acta. Crystal.* **1967**, *23*, 334.

[12] I. E. Grey, C. Li, I. C. Madsen and G. Braunshausen, *Mat. Res. Bull.* **1988**, *23*, 743-753.

[13] J.-E. Jorgensen, D. J. Jorgensen, B. Batlogg, J. P. Remeika and J. D. Axe, *Phys. Rev. B*, **1986**, *33*, 4793-4798.

[14] A. Norotsky, J. C. Jamieson and O. J. Kleppa, *Science* **1967**, *54*, 1447.

[15] H. Z. Zhang and J. F. Banfield, *J. Mater. Chem.* **1998**, *8*, 2073.

[16] H. Z. Zhang and J. F. Banfield, *J. Phys. Chem. B* **2000**, *104*, 3481.

[17] *Kronos International* **1996**.

[18] G. V. Samsonov, *The Oxide Handbook*, IFI/Plenum Press, New York, **1982**.

[19] U. Diebold, *Surf. Sci. Rep.* **2003**, *48*, 53-229.

[20] H. A. Macloeod, *Thin Film Opticl Filters 2nd ed*, MacMillan, New York, **1986**.

[21] W. D. Brown and W. W. Granneman, *Solid State Electron.* **1978**, *21*, 837.

[22] Y. Matsumoto, T. Shono, T. Hasegawa, T. Fukumura, K. Kawasaki and P. Ahmet, *Science* **2001**, *291*, 854.

[23] P. T. Moseley and B. C. Tofield, *Solid State Gas Sensors*, Adam Hilger, **1987**.

[24] D. E. MacDonald, N. Deo, B. Markovic, M. Stranick and P. Somasundaran, *Biomaterials* **2002**, *23*, 1269.

[25] L. Kavan, D. Fattakhova and P. Krtil, *J. Electrochem. Soc.* **1999**, *146*, 1375.

[26] L. Kavan, M. Kalbáč, M. Zukalová, I. Exnar, V. Lorenzen, R. Nesper and M. Graetzel, *Chem. Mater.* **2004,** *16,* 477-485.

[27] L. Kavan, M. Kalbáč, M. Zukalová, I. Exnar, V. Lorenzen, R. Nesper and M. Graetzel, *Chem. Mater.* **2005,** *17,* 1248-1255.

[28] B. O'Regan and M. Grätzel, *Nature* **1991**, *353*, 737.

[29] A. Fujishima and K. Honda, *Nature* **1972**, *238*, 37.

[30] R. Wang, K. Hashimoto, A. Fujishima, M. Chikuni, E. Kojima and A. Kitamura, *Nature* **1997**, 388, 431.

[31] S. N. Frank and A. J. Bard, *J. Am. Chem. Soc.* **1977**, *81*, 1484.

[32] T. Matsunaga, R. Tomato, T. Nakajima and H. Wake, *FEMS Microbiol. Lett.* **1985**, *29*, 211.

[33] A. Fujishima, J. Ohtsuki, T. Yamashita and S. Hayakawa, *Photomed. Photobiol.* **1986**, *8*, 45.

[34] G. N. Schrauzer and T. D. Guth, *J. Am. Chem. Soc.* **1977**, *99*, 303.

[35] A. Sclafani and J. M. Herrmann, *J. Phys. Chem.* **1996,** *100,* 13655-13661.

[36] Z. Zhang, C. C. Wang, R. Zakaria, and J. Y. Ying**,** *J. Phys. Chem. B* **1998,** *102,* 10871-10878.

[37] M. Anpo, T. Shima, S. Kodama, and Y. Kubokawa, *J. Phys. Chem.* **1987,** *91,* 4305-4310.

[38] A. L. Linsbigler, G. Q. Lu and J. T. Yates, *Chem. Rev.* **1995**, *95*, 735.

[39] R. Tompson, *Industrial inorganic chemicals: production and uses.* The Royal Society of Chemistry **1995**.

[40] K. L. Choy, *Prog. Mater. Sci.* **2003**, *48*, 57.

[41] R. van de Krol, A. Goossens and J. Schoonman, *J. Electrochem. Soc.* **1997**, *144*, 1723.

[42] A. Smith and R. Rodriguez-Clemente, *Thin Solid Films* **1999**, *345*, 192.

[43] S. K. Poznyak, A. I. Kokorin and A.I. Kulak, *J. Electroanal. Chem.* **1998**, *442*, 99.

[44] S. Yin, Y. Fujishiro, J. Wu, M. Aki and T. Sato, *J. Mater. Proc. Tech.* **2003**, *137*, 45.

[45] U. Bach, D. Lupo, P. Comte, J. E. Moster, F. Weissortel and J. Salbeck, *Nature* **1998**, *395*, 583.

[46] K. T. Lim, H. S. Hwang, W. Ryoo and K. P. Johnson, *Lanmuir* **2004**, *20*, 2466.

[47] N. Nagaveni, M. S. Hedge, N. Ravishankar, G. N. Subbanna and G. Madras, *Lanmuir* **2004**, *20*, 2900.

[48] L. Kavan, B. O'Regan, A. Kay and M. Grätzel, *J. Electroanal. Chem.* **1993**, *346*, 291.

[49] J. P. Jolivet, *De la solution à l'oxide*, CNRS Édition **1994**.

[50] S. Anderson and A. D. Wadsley, *Acta Crys.* **1961**, *14*, 1245.

[51] H. Dresdner and M. J. Buerger, *Z. für Krist.* **1962**, *117*, 441.

[52] A. Oles, A. Szytula and A. Wanic, *Physica Status Solidi* **1970**, *41*, 173-177.

[53] I. E. Grey, I. C. Madsen, J. A. Watts, L. A. Bursill and J. Kwiatkowska, *J. Solid State Chem*. **1985**, *58*, 350-356.

[54] J. Kwiatkowska, *Acta. Cryst.* **1968**, *24*, 392-396.

[55] M. Dion, Y. Piffard and M. Tournoux, *J. Inorg. Nucl. Chem.* **1978**, *40*, 917.

[56] A. Verbaere and M. Tournoux, Bulletin de la Société Chemique de France **1973**, 1237-1241.

[57] Watts, *J. Solid State Chem.* **1970**, *1*, 319-325.

[58] T. Sasaki, M. Watanabe, Y. Fujiki, Y. Kitami and M. Yokoyama, *J. Solid State Chem.* **1976**, *17*, 431.

[59] A. D. Wedsley and W. G. Mumme, *Acta Crys.* **1968**, *24*, 392-396.

[60] E. Anderson, I. Anderson and E. Skou, *Solid State Ionics*, **1988**, *27*, 81.

[61] J. Schmachtel and H. Mueller-Buschbaum, *Zeitschrift für Anorganische und Allgemeine Chemie* **1977**, *435*, 243-246.

[62] S. Andersson and A. D.Wadsley, *Acta. Crystal.* **1962**, *15*, 194.

[63] M. Hervieu, G. Desgardin and B. Raveau, *J. Solid State Chem.* **1979**, *30*, 375-384.

[64] I. Keeman, *Z. Anorg. Allg. Chem.* **1966**, *346*, 30.

[65] K. Wefers, *Naturwissenschaften* **1967**, *54*, 19.

[66] M. Wanabe, *J. Solid State Chem.* **1981**, *36*, 91-96.

[67] S. Iijima, Nature 1991, 354, 56.

[68] N. G. Chopra, R. J. Luyken, K. Cherry, V. H. Crespi, M. L. Cohen, S. G. Louie, A. Zettl, *Science* **1995**, *269*, 966.

[69] M. Niederberger, H. J. Muhr, F. Krumeich, F. Bieri, D. Gunther and R. Nesper, *Chem. Mater.* **2000**, *12*, 604.

[70] B. C. Satishkumar, A. Govindaraj, E. M. Voli, L. Basumallic, C. N. R. Rao, *J. Mater. Res.* **1997**, *12*, 604.

[71] T. Kasuga, M. Hiramatsu, A. Hoson, T. Sekino and K. Niihara *Langmuir* **1998,** *14,* 3160-3163.

[72] T. Kasuga, M. Hiramatsu, A. Hoson, T. Sekino and K. Niihara *Adv. Mater.* **1999**, 11, 1307-1311.

[73] Q. Chen, W. Zhou, G. H. Du and L. M. Peng, *Adv. Mater.* **2002**, *14*, 1208-1211.

[74] Q. Chen, G.H. Du, S. Zhang and L.-M. Peng, *Acta Cryst.* **2002**, *B58*, 587-593.

[75] Y.Q. Wang, G.Q. Hu, X.F. Duan, H.L. Sun, Q.K. Xue, *Chem. Phys. Lett.* **2002**, *365*, 427–431.

[76] B. D. Yao, Y. F. Chan, X. Y. Zhang, W. F. Zhang, Z. Y. Yang, and N. Wang, *Appl. Phys. Lett.* **2003**, *82*, 281-283.

[77] R. Ma, Y. Bando, T. Sasaki, *Chem. Phys. Lett.* **2003**, *380*, 577–582.

[78] J. Yang, Z. Jin, X. Wang, W. Li, J. Zhang, S. Zhang, X. Guo and Z. Zhang, *Dalton Trans.* **2003**, 3898-3901.

[79] W. Wang, O. K. Varghese, M. Paulose, and C. A. Grimes, Q. Wang and E. C. Dickey, *J. Mater. Res.* **2004**, 19, 417-422.

[80] D. V. Bavykin, V. N. Parmon, A. A. Lapkin and F. C. Walsh, *J. Mater. Chem.* **2004**, *14*, 3370-3377.

[81] Á. Kukovecz, M. Hodos, E. Horváth, G. Radnóczi, Z. Kónya, and I. Kiricsi, *J. Phys. Chem. B* **2005,** *109,* 17781-17783.

[82] C. C. Tsai and H. Teng, *Chem. Mater.* **2006,** *18,* 367-373.

[83] Y. F.Chen, C. Y. Lee, M. Y. Yeng, H. T. Chiu, *Mater. Chem. Phys.* **2003**, *81*, 39–44.

[84] Z. Y. Yuan, W. Zhou and B. L. Su, *Chem. Comm.* **2002**, 1202-1203.

[85] A. R. Armstrong, G. Armstrong, J. Canales, and P. G. Bruce, *Angew. Chem. Int. Ed.* **2004**, *43*, 2286 –2288.

[86] H. Zhu, X. Gao, Y. Lan, D. Song, Y. Xi and J. Zhao, *J. Am. Chem. Soc.* **2004**, *126*, 8380-8381.

[87] C. C. Tsai and H. Teng, *Chem. Mater.* **2004,** *16,* 4352-4358.

[88] X. Sun and Y. Li, *Chem. Eur. J.* **2003**, *9*, 2229-2238.

[89] L. Wang, G. Li and Z. Zhang, *Mater. Res. Bull.* **2006**, *41*, 842–846.

[90] X. Ma, C. Feng, Z. Jin, X. Guo, J. Yang and Z. Zhang, *Journal of Nanoparticle Research* **2005**, *7*, 681–683.

[91] Y. Zhou, L. Cao, F. Zhang, B. He and H. Li, *J. Electrochem. Soc.* **2003**, *150,* A1246-A1249.

[92] J. Li, Z. Tang and Z. Zhang, *Electrochem. Comm.* **2005**, *7*, 62–67.

[93] G. Armstrong, A. R. Armstrong, J. Canales and P. G. Bruce, *Chem. Comm.* **2005**, 2454–2456.

[94] M. Zhang, Z. Jin, J. Zhang, X. Guo, J. Yang, W. Li, X. Wang, Z. Zhang, *J. Mol. Catal. A* **2004**, *217*, 203–210.

[95] H. Tokudome and M. Miyauchi, *Chem. Lett.* **2004**, *33*, 1108-1109.

[96] S. H. Chien, Y. C. Liou and M. C. Kuo, *Synthetic Metals* **2005**,*152*, 333–336.

[97] M. Hodos, E. Horváth, H. Haspel, Á. Kukovecz, Z. Kónya, I. Kiricsi, *Chem. Phys. Lett.* **2004**, *399*, 512–515.

[98] Y. Ohsaki, N. Masaki, T. Kitamura, Y. Wada, T. Okamoto, T. Sekino, K. Niiharab and S. Yanagida, *Phys. Chem. Chem. Phys.* **2005**, *7*, 4157 – 4163.

[99] D.V. Bavykin, A. A. Lapkin, P. K. Plucinski, J. M. Friedrich, and F. C. Walsh, *J. Phys. Chem. B* **2005,** *109,* 19422-19427.

[100] S. H. Lim, J. Luo,. Z. Zhong, W. Ji and J. Lin, *Inorg. Chem.* **2005**, *44*, 4124-4126.

[101] L. Qian, Z. S. Jin, S. Y.Yang, Z. L. Du, and X.R. Xu, *Chem. Mater.* **2005,** *17,* 5334-5338.

[102] H. Sutrisno, *Ph.D thesis* **2002,** IMN, Unversité de Nantes.

[103] A. Rouet, *Ph.D thesis* **2005,** IMN, Unversité de Nantes.

[104] L. Brohan, *Ph.D thesis* **1986**, Unversité de Nantes.

[105] M. Mancini-Le Granvalet, *Ph.D thesis* **1994,** IMN, Unversité de Nantes.

[106] D. Brunet, *Ph.D thesis* **1994,** IMN, Unversité de Nantes.